CILAMCE 2017

Florianópolis - Santa Catarina - Brazil

IMPLEMENTATION OF RHEOLOGICAL MODELS TO DESCRIBE THE VISCOELASTIC CREEP BEHAVIOR BASED ON THE POSITIONAL FINITE ELEMENT METHOD

Becho, Juliano dos Santos

Barros, Felício Bruzzi

Greco, Marcelo

julianobecho@dees.ufmg.br

felicio@dees.ufmg.br

mgreco@dees.ufmg.br

Structural Engineering Graduate Program, Federal University of Minas Gerais, School of Engineering

Av. Presidente Antônio Carlos, 6627 / Room Office 4127, Belo Horizonte - MG, Zip-Code: 31270-901, Brazil

Abstract. *This paper presents the formulations and computational implementations of four different rheological models applied to the description of the viscoelastic creep behavior due to the application of a static loading. The formulations are based on the Positional Finite Element Method, developed for analysis of space truss elements. The stress-strain relations required in the formulations are obtained through rheological models, physically described by springs and dashpots associations. These relations, called rheological relations, take into account the time variable and are used to describe the viscoelastic behavior of the elements. The different formulations developed using the rheological relations for the Maxwell, Kelvin-Voigt, Boltzmann and Zener models are then presented and numerically implemented. As an example, a bar under traction is analyzed using the implementations developed with each model. The responses obtained for deformation along time under constant stress (creep phenomena) are compared among themselves and regarding the respective behaviors expected by the theory of viscoelasticity. The results confirm the capacity of the Positional Finite Element Method to describe different creep behaviors through the adoption of appropriate rheological relation. Furthermore, the behavior of a space truss structure is simulated with different models and the results are analyzed and discussed in light of the viscoelasticity and structure theories.*

Keywords: *Creep, Viscoelasticity, Positional Finite Element Method, Rheological Model, Truss*

1 INTRODUCTION

On a structural project, one of the fundamental problems is to find a solution that presents a good performance (a predictable and safe structure) with low economic cost. With this purpose, many works have been devoted to the study and modeling of the behavior of unconventional materials in many different areas, such as infrastructure, civil construction, mechanical industry and aerospace industry. The works of Godat *et al*. (2013), Kästner *et al*. (2012), Sá *et al*. (2011a) and Muñoz-Rojas *et al*. (2011) are good examples.

Among other unconventional materials used in recent researches regarding structural analysis, we point out the polymeric materials and the composite materials with polymeric matrix, especially for presenting a good strength/stiffness ratio in comparison to conventional structural materials. On the other hand, in general these materials present viscoelastic or viscoelastoplastic mechanical behavior depending on their properties and the stress levels that they are exposed. These behaviors are characterized by their dependence of time in response to external exposures, and are described by the combination of viscous behavior, characteristic of fluid materials, and elastic or plastic behavior, characteristic of solid materials (Findley *et al*., 1989).

The interests of some of the recent researches related to viscoelastic and viscoelastoplastic behavior are focused on the development of numerical formulations that adopt phenomenological equations, based on rheological models, to represent the relation between the stress, strain and time; and also on parameter fitting techniques for these models, as pointed out in the following works.

Mesquita and Coda (2003) propose a formulation of the Boundary Element Method for the analysis of three-dimensional solids with viscoelastic behavior, considering the Kelvin-Voigt and Boltzmann rheological models. A similar formulation is adopted in Panagiotopoulos *et al*. (2014) to compare the responses of the Hooke, Kelvin-Voigt and Boltzmann solid models, which respectively represent the instantaneous elastic, damped elastic and creep behaviors. Besides these, the responses of the fluid models of Maxwell, Jeffreys and Burgers were also implemented and compared.

Liu *et al*. (2008) propose a formulation based on integral equations for describing the nonlinear viscoelastic behavior of polyethylene for structural applications. The viscoelastic behavior is considered by adopting the generalized model of Kelvin-Voigt and the respective parameters are obtained through a methodology based on linear interpolation. A similar formulation is adopted in Kühl *et al*. (2016) to describe the viscoelastic behavior of High Density Polyethylene. For the viscoelastic part of the strain, a generalized model of Kelvin-Voigt is adopted, and, for the viscoelastoplastic part, the equation of Zapas-Crissman is considered. The viscoelastic parameters are obtained through a curve fitting based on the method of Particle Swarm Optimization, whereas the viscoplastic parameters are obtained through a linear regression of the Least Squares Method.

Semptikovski and Muñoz-Rojas (2013) propose a tridimensional formulation of the Finite Element Method using a simplified beam element. In this work the linear viscoelastic behavior in elements made of High Density Polyethylene is considered from a generalized Maxwell rheological model, based on Kaliske and Rothert (1997).

Carniel *et al*. (2015) propose a formulation of the Finite Element Method to analyze spatial truss with viscoelastic and viscoelastoplastic behavior including mechanical degradation. The generalized rheological model of Kelvin-Voigt was adopted for the description of viscoelastic behavior, whereas the viscoplastic behavior was considered by using the equation of Perzyna. The degradation of the material was considered by using the damage model of Lemaitre. The parameters of the material were obtained through a curve fitting based on the Particle Swarm Optimization.

Becho *et al*. (2015) proposed a formulation based on the Positional Finite Element Method for the description of the creep viscoelastic behavior in plane frame structures, taking into account the beams kinematics of Bernoulli-Euler. In this case, the contribution of creep is introduced from the rheological relation obtained from the Zener model. A similar formulation is adopted in Becho *et al*. (2016) to describe the mechanical viscoelastic behavior in traction bars considering also the Zener rheological model. Such formulation is then employed for the simulation of creep-recovery tests of bars made of High Density Polyethylene.

As noted, different methods or formulations may be used to describe a particular structural behavior depending essentially on the analyzed problem features. The models adopted to describe the mechanical behavior depend on the constituent materials of the analyzed structural components. Thus, different models can be adopted for each kind of mechanical response analyzed in order to represent with better or worse approximation regarding the actual behavior of the material. For example, mechanical responses of fluid materials may be better represented by models such as Maxwell, Jeffreys and Burger, on the other hand solid materials may be better represented by models such as Hooke, Kelvin-Voigt, Zener, and Boltzmann.

In this context, a numerical formulation developed based on the Positional Finite Element Method, analogous to that presented in Becho *et al*. (2016), is used to implement four different rheological models able to describing viscoelastic behavior. In this work, the formulation is particularized to describe the creep viscoelastic behavior (strain variation over time when exposed to constant stress) due to the application of a static loading (inertial forces are not considered) in space truss finite elements, adopting a measure of engineering deformation. The models presented and implemented numerically are Maxwell, Kelvin-Voigt, Boltzmann and Zener.

This work is divided into four main parts. Initially, the general formulation of the Positional Finite Element Method is presented. Subsequently, the particularities of the truss elements are presented and introduced into the formulation. Then, the models and rheological relations implemented are presented. Finally, the formulation is particularized for each rheological model implemented.

As an example, a bar under traction is analyzed using the implementations developed with each model in order to confirm the capacity of the Positional Finite Element Method to describe different creep behaviors through the adoption of appropriate rheological relation. The responses obtained for deformation along time under constant stress (creep phenomena) are compared among themselves and regarding the respective behaviors expected by the theory of viscoelasticity. Furthermore, the behavior of a space truss structure is simulated with the different models and the results are analyzed and discussed in light of the viscoelasticity and structure theories.

2 POSITIONAL FINITE ELEMENT METHOD

The Positional Finite Element Method used for this work is based on the formulation found in Greco *et al.* (2006), which was developed to analyze space truss structures with physical and geometrical nonlinearities. This formulation considers the nodal positions of a structure as variables, rather than nodal displacements, regarding a system of reference fixed in the space in order to describe the kinematics of the finite elements. The method was selected due to its efficiency for applications and developments, as shown in recent researches concerning the nonlinear numerical analysis, besides being supported by physics principles based on energy equilibrium that are both consistent and easy to understand.

In this item, the general formulation of the Positional Finite Element Method is initially presented. Subsequently, the particularities of the space truss elements are presented and introduced into the formulation. However, for the moment no mention is made regarding the rheological model and the constitution of the material.

2.1 General formulation

The Positional Finite Element Method is based on principles of energy balance, more specifically on the equilibrium of total potential energy. In general, from the Principle of Virtual Work, the functional of the total potential energy for a conservative and static structural system can be described as

$$\Pi = U - P \ , \tag{1}$$

where U is the strain energy expressed by

$$U = \int_V u dV = \int_V \int_\varepsilon \sigma(\varepsilon)\, d\varepsilon\, dV \ , \tag{2}$$

defined by the integral of the specific strain energy u in an initial reference volume V, in which $\sigma(\varepsilon)$ represents the stress field according to the constitutive or rheological relation of the material as a function of the strain field ε. P is the potential energy of the external forces expressed by

$$P = \sum F_i X_i \ , \tag{3}$$

in which the degrees of freedom, considering a space truss element with two nodes and three degrees of freedom per node, can be represented by $X_i = (X_1, Y_1, Z_1, X_2, Y_2, Z_2)$ for $i = (1, 2, 3, 4, 5, 6)$ and the respective nodal static loads for the two degree of freedom represented by $F_i = (F_{X1},\ F_{Y1},\ F_{Z1},\ F_{X2},\ F_{Y2},\ F_{Z2})$.

Applying the principles of the variational approach to obtain the stationary configuration, the one that corresponds to the minimum (or maximum) value of the functional of the total potential energy, the first variation of Eq. (1) must vanish (Dym and Shames, 2013), that is

$$\delta^{(1)}\Pi = 0 \ . \tag{4}$$

Regarding the variation of nodal positions, which are the unknown variables, one has

$$\delta^{(1)}\Pi = \frac{\partial \Pi}{\partial X_i}\delta X_i = 0\,. \tag{5}$$

Since δX_i might assume any arbitrary values, one has

$$\frac{\partial \Pi}{\partial X_i} = \frac{\partial U}{\partial X_i} - \frac{\partial P}{\partial X_i} = 0\,. \tag{6}$$

This equation represents the principle of stationary total potential energy (Crisfield, 1991), which provides the equilibrium position of the structure. So, the structural equilibrium will occur when the derivative of the total potential energy, in relation to the nodal parameters, is null, that is, when the variation rate of the total potential energy is null. It is important to note that, for this kind of structural problem, this condition provides the minimum value for the functional of the total potential energy.

Equation (6) is a system of six equations (three degrees of freedom to each one of the two nodes that define a space truss element) and represents a nonlinear system of equations. As the relationship between the total strain energy, U, and nodal parameters, X_i, is nonlinear. Then, it must be solved using a proper method to solve systems of equations. Thus, the appropriate solution of the system of equations gives the equilibrium nodal positions of the structure. In this work, it is solved using the iterative method of Newton-Raphson, briefly described below.

Writing Eq. (6) in a compact form

$$\frac{\partial \Pi}{\partial X_i} = g_i(X) = 0\,. \tag{7}$$

Then, expanding in Taylor series truncated in linear terms, one has

$$g_i(X) \cong g_i(X^0) + g_{i,k}(X^0)\Delta X_k \cong 0\,, \qquad (i,k = 1,2,\dots,n) \tag{8}$$

where n is the number of degrees of freedom, X^0 represents the trial vector position, $g_i(X^0)$ represents the terms of residues vector, $g_{i,k}(X^0)$ represents the terms of Hessian matrix and ΔX_k represents the terms of nodal positions correction vector. Wherein, $g_i(X^0)$ and $g_{i,k}(X^0)$ can be obtained respectively as follow

$$g_i(X^0) = U_{,i} - F_i\,, \tag{9}$$

$$g_{i,k}(X^0) = U_{,ik}\;. \tag{10}$$

Then, iterative Newton-Raphson procedure can be summarized as follow:

(1) Assuming X^0 as the initial configuration, calculate $g_i(X^0)$ following Eq. (9);

(2) For this X^0, calculate the Hessian matrix following Eq. (10);

(3) Solve the system of Eq. (8) and determine ΔX;

(4) Update position $X^0 = X^0 + \Delta X$;

(5) Return to step 1 until ΔX is sufficiently small.

2.2 Formulation of the Positional Finite Element Method for space trusses

From the general formulation of item 2.1 it is possible to note that the particularization of the formulation may be simply performed by the proper development of total strain energy, U, regarding the implemented finite element. Then, aiming to define the adequate expression to represent the total strain energy it is necessary to understand the kinematic of the finite element to be studied and its relation with the adopted strain measure.

In this work, it is adopted the truss finite element. In this formulation each finite element has its geometry mapped out by the parametrization in function of the dimensionless variable ξ (ranging from 0 to 1) as shown in Fig. 1. X_1, Y_1 and Z_1 are the initial node parameters (initial node coordinates) and X_2, Y_2 and Z_2 are the final node parameters (final node coordinates) of the finite element. These parameters represent the degrees of freedom in each node.

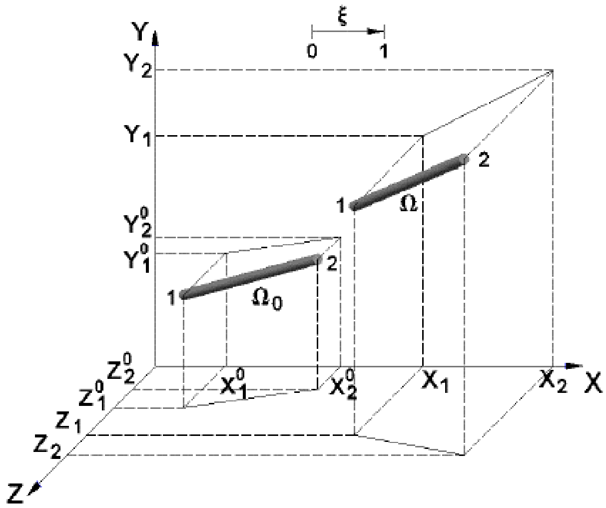

Figure 1: Parametrization of a truss finite elements (*Ω_0* is the initial configuration and *Ω* is the deformed configuration)

From Figure 1 it is possible to write the parametric equations of the element as

$$x = X_1 + (X_2 - X_1)\xi \; , \tag{11}$$

$$y = Y_1 + (Y_2 - Y_1)\xi \; , \tag{12}$$

$$z = Z_1 + (Z_2 - Z_1)\xi \; . \tag{13}$$

The engineering strain measure as defined in Ogden (1997) can be represented by

$$\varepsilon = \frac{ds - ds^0}{ds^0} = \frac{\dfrac{ds}{d\xi} - \dfrac{ds^0}{d\xi}}{\dfrac{ds^0}{d\xi}} \; , \tag{14}$$

where $ds/d\xi$ represents the length of the element in a deformed configuration and $ds^0/d\xi$ represents its length in a non-deformed configuration, respectively defined as

$$\frac{ds}{d\xi} = \sqrt{\left(\frac{dx}{d\xi}\right)^2 + \left(\frac{dy}{d\xi}\right)^2 + \left(\frac{dz}{d\xi}\right)^2} = \sqrt{(X_2 - X_1)^2 + (Y_2 - Y_1)^2 + (Z_2 - Z_1)^2} = l \,, \tag{15}$$

$$\frac{ds^0}{d\xi} = \sqrt{\left(\frac{dx^0}{d\xi}\right)^2 + \left(\frac{dy^0}{d\xi}\right)^2 + \left(\frac{dz^0}{d\xi}\right)^2} = \sqrt{(X_2^0 - X_1^0)^2 + (Y_2^0 - Y_1^0)^2 + (Z_2^0 - Z_1^0)^2} = l^0 \,. \tag{16}$$

Then, the total strain ε can be written as follows

$$\varepsilon = \frac{\sqrt{B}}{l^0} - 1 \,, \tag{17}$$

where l^0 is the initial length of the element, and B is defined as

$$B = (X_2 - X_1)^2 + (Y_2 - Y_1)^2 + (Z_2 - Z_1)^2 \,. \tag{18}$$

Considering truss finite elements with invariant cross-section area A, and considering a simple mapping in the dimensionless variable ξ, showed in Fig. 1, it is possible to perform the integration of Eq. (2) along the length of the finite element as

$$U = l^0 A \int_0^1 \int_\varepsilon \sigma(\varepsilon)\, d\varepsilon\, d\xi \,. \tag{19}$$

Thus, the total strain energy can be obtained by adopting a proper stress-strain relation in Eq. (19), since the strain measure is defined by Eq. (17). This relation depends essentially on the constituent materials, and in this work it is derived by rheological models.

3 IMPLEMENTATION OF RHEOLOGICAL MODELS

One of the main characteristics in a structural analysis is the adoption of a constitutive or rheological relation that represents, in an appropriate way, the behavior of the material (Findley *et al.*, 1989). Therefore, following Mesquita and Coda (2003) and Panagiotopoulos *et al.* (2014), the rheological relations that represents the viscoelastic materials are deduced from rheological models, based on the expected creep behavior. Having this in mind, four different rheological models able to describe viscoelastic behavior are implemented using the described Positional Finite Element Method. Initially, the rheological models are presented and then the formulation is particularized for each rheological model implemented.

3.1 Definition of the rheological relations

In this item, the four adopted rheological models are presented, as well as their equations that relate stress, strain and time. The models presented and implemented numerically are Maxwell, Kelvin-Voigt, Boltzmann and Zener, physically described by springs and dashpots associations, Fig 2. The rheological relations for these models can be derived by total stress-strain relation provided by each model and the individual stress-strain relations of each model component. The developments of these relations are described in detail in Findley *et al.* (1989) and Marques and Creus (2012).

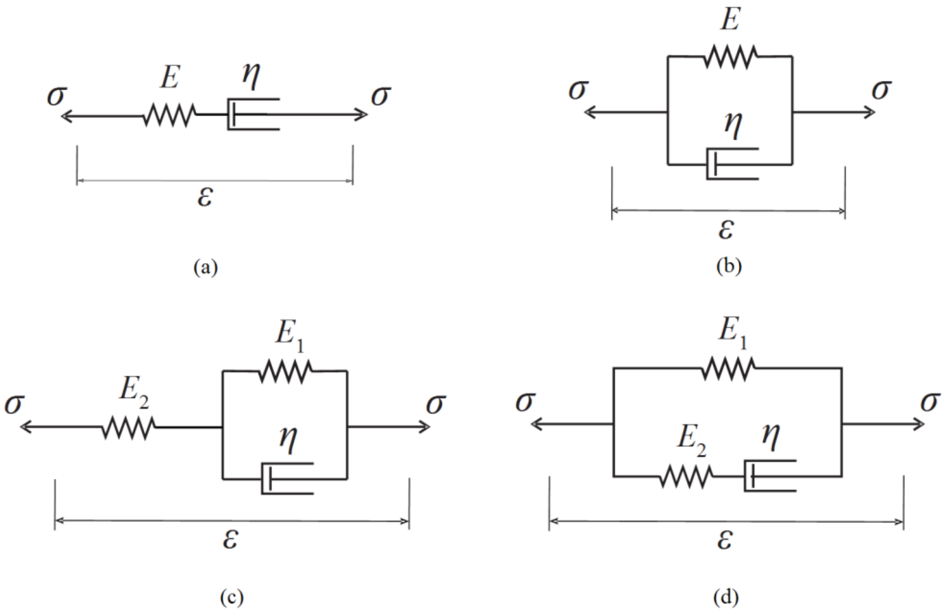

Figure 2: (a) Maxwell model; (b) Kelvin-Voigt model; (c) Boltzmann model; (d) Zener model

The four models are able to describe the creep viscoelastic behavior (characterized by the strain variation over time when exposed to constant stress), but with some particularities briefly described below.

For all described models, σ and ε form the conjugated pair of stress and strain engineering, treated as scalar, since it is restricted to the analysis of one-dimensional finite elements. Whereas, $\dot{\sigma}$ and $\dot{\varepsilon}$ represent, respectively, the variation rates of stress and strain over time. Furthermore, E, E_1, E_2 and η are physical parameters that represent the mechanical proprieties of the materials.

Maxwell model. This model is able to describe an instantaneous elastic behavior followed by a viscous behavior with constant strain rate, typical of fluid materials. Theoretically, the viscoelastic strain increase indefinitely. It can be represented physically by a two-parameter model constituted by a spring and a dashpot associated in series (Marques and Creus, 2012), as showed in Fig 2 (a).

In the Fig 2(a), it is important to note that the parameter E determine the instantaneous elastic behavior and represents the elasticity module of the material. Moreover, parameter η represents viscosity module of the material, which determines the strain rate over time.

The rheological relation can be represented by

$$\sigma = \eta\dot{\varepsilon} - \frac{\eta}{E}\dot{\sigma} \,. \tag{20}$$

Kelvin-Voigt model. This model is not able to describe an instantaneous elastic behavior, describing a damped elastic behavior with decreasing strain rate, typical of solid materials. For a sufficiently large period of time, the damped elastic strain tends to the instantaneous elastic strain response expected by a linear elastic material. It can be represented physically by a two-parameter model constituted by a spring and a dashpot associated in parallel (Marques and Creus, 2012), as showed in Fig 2 (b).

In the Fig 2(b), it is important to note that the parameter E determines the final strain tending after a sufficiently large period of time, and represents the elasticity module of the material in the damped elastic behavior. Moreover, parameter η represents viscosity module of the material, which determines the strain rate over time and provides a damped behavior to the material.

The rheological relation can be represented by

$$\sigma = E\varepsilon + \eta\dot{\varepsilon} \; . \tag{21}$$

Boltzmann model. This model is able to describe an instantaneous elastic behavior followed by a viscoelastic behavior with decreasing strain rate, typical of solid materials. For a sufficiently large period of time, the viscoelastic strain tends to a prescribed strain defined by viscoelastic material parameters. It can be represented physically by a three-parameter model constituted by a spring associated in series with a Kelvin-Voigt arrangement (spring and dashpot associated in parallel) (Marques and Creus, 2012), as showed in Fig 2 (c).

In the Fig 2(c), it is important to note that the parameter E_2 determines instantaneous elastic behavior and represents the elasticity module of the material. Parameter E_1 determines the increase in total strain over time, and represents the elasticity module of the material in the viscoelastic behavior. Moreover, parameter η represents viscosity module of the material, which determines the strain rate over time and provides a damped behavior to the material.

The rheological relation can be represented by

$$\sigma = \frac{E_1 E_2}{E_1 + E_2}\varepsilon + \frac{\eta E_1}{E_1 + E_2}\dot{\varepsilon} - \frac{\eta}{E_1 + E_2}\dot{\sigma} \; . \tag{22}$$

Zener model. This model is able to describe an instantaneous elastic behavior followed by a viscoelastic behavior with decreasing strain rate, typical of solid materials. For a sufficiently large period of time, the viscoelastic strain tends to a prescribed strain defined by viscoelastic material parameters. It can be represented physically by a three-parameter model constituted by a spring associated in parallel with a Maxwell arrangement (spring and dashpot associated in series) (Marques and Creus, 2012), as showed in Fig 2 (d).

In the Fig 2(d), it is important to note that the parameters E_1 and E_2 determine instantaneous elastic behavior, where the sum of these parameters represents the elasticity module of the material. Parameter E_1 determines the final strain tending (the sum of the instantaneous elastic strain and the damped elastic strain) after a sufficiently large period of time, and represents the elasticity module of the material in the viscoelastic behavior. Moreover, parameter η represents viscosity module of the material, which determines the strain rate over time and provides a damped behavior to the material.

The rheological relation can be represented by

$$\sigma = E_1\varepsilon + \frac{\eta(E_1 + E_2)}{E_2}\dot{\varepsilon} - \frac{\eta}{E_2}\dot{\sigma} \; . \tag{23}$$

3.2 Development of the formulation for each rheological model

In order to develop the formulation described in item 2 taking into account the rheological model and the constitution of the materials, the total strain energy U, described by Eq. (19), can be rewritten using the stress-strain relations presented in item 3.1, since the strain measure ε is defined by Eq. (17).

Thus, in this item, the particularization of the total strain energy and its derivatives will be presented for each rheological model implemented. For this purpose, the following definitions are considered respectively for the strain rate $\dot{\varepsilon}$ and for the infinitesimal strain $d\varepsilon$:

$$\dot{\varepsilon} = \frac{d\varepsilon}{dt} = \frac{d\varepsilon}{dX_i}\frac{dX_i}{dt} = \varepsilon_{,i}\dot{X}_i \ , \tag{24}$$

$$d\varepsilon = \varepsilon_{,i}\, dX_i \ , \tag{25}$$

where $\varepsilon_{,i}$ is the derivative of Eq. (17) in relation to the degrees of freedom and $\dot{X}_i$ represents the velocity of the positional variation in the direction of each one of the six degrees of freedom.

The definition introduced by Eq. (24) is important because in the positional formulation used, based on nodal positions, it is simpler to obtain the rate of change of the nodal positions with time than the rate of change of the deformations with time. Moreover, the definition introduced by Eq. (25) is important to perform a change of variables and represent the integral of the Eq. (19) in relation to degrees of freedom.

To compute the velocity of the positional variation an auxiliary variable, $\dot{X}_{axial}$, can be used to describe the approximated variation of the finite element length at a time variation Δt, as described by

$$\dot{X}_{axial} = \frac{1}{\Delta t}\left(\sqrt{B_s} - \sqrt{B_{s-1}}\right) , \tag{26}$$

where the subscript s is related to the calculation regarding the current nodal positions and $s-1$ is related to the calculation regarding the previous nodal positions. Thus, the terms of the velocity of positional variation in each degree of freedom can be obtained by means of an appropriate matrix of transformation from the local (axial) system to the global system. In this approach, considering constant time intervals, temporal integrations are not required.

Using Eqs. (17) - (23), it can be represented the total strain energy and its first and second derivatives regarding the nodal parameters ($U_{,i}$ and $U_{,ik}$) for each rheological model as stated below:

Maxwell model. Using Eqs. (17), (19) and (20), one has

$$U = \int_0^1 \left[\int_{X_i} \frac{\eta A}{4l^0}\left(\frac{B_{,i}{}^2}{B}\right)\dot{X}_i dX_i - \int_{X_i} \frac{\eta A}{2E}\left(\frac{B_{,i}}{\sqrt{B}}\right)\dot{\sigma} dX_i \right] d\xi \ , \tag{27}$$

$$U_{,i} = \int_0^1 \left[\frac{\eta A}{4l^0} \left(\frac{B_{,i}{}^2}{B} \right) \dot{X}_i - \frac{\eta A}{2E} \left(\frac{B_{,i}}{\sqrt{B}} \right) \dot{\sigma} \right] d\xi \ , \tag{28}$$

$$\begin{aligned} U_{,ik} = \int_0^1 \Bigg[& \frac{\eta A}{4l^0} \left(\frac{B_{,i}{}^2 \dot{X}_{i,k}}{B} + \frac{2B_{,i}\, B_{,ik}\, \dot{X}_i}{B} - \frac{B_{,i}{}^2\, B_{,k}\, \dot{X}_i}{B^2} \right) + \\ & - \frac{\eta A}{2E} \left(\frac{B_{,ik}}{\sqrt{B}} - \frac{B_{,i}\, B_{,k}}{2B\sqrt{B}} \right) \dot{\sigma} \Bigg] d\xi \ . \end{aligned} \tag{29}$$

Kelvin-Voigt model. Using Eqs. (17), (19) and (21), one has

$$U = \int_0^1 \left[\frac{EAl^0}{2} \left(\frac{\sqrt{B}}{l^0} - 1 \right)^2 + \int_{X_i} \frac{\eta A}{4l^0} \left(\frac{B_{,i}{}^2}{B} \right) \dot{X}_i dX_i \right] d\xi \ , \tag{30}$$

$$U_{,i} = \int_0^1 \left[\frac{EA}{2} \left(\frac{B_{,i}}{l^0} - \frac{B_{,i}}{\sqrt{B}} \right) + \frac{\eta A}{4l^0} \left(\frac{B_{,i}{}^2}{B} \right) \dot{X}_i \right] d\xi \ , \tag{31}$$

$$\begin{aligned} U_{,ik} = \int_0^1 \Bigg[& \frac{EA}{2} \left(\frac{B_{,i}\, B_{,k}}{2B\sqrt{B}} + \frac{B_{,ik}}{l^0} - \frac{B_{,ik}}{\sqrt{B}} \right) + \\ & + \frac{\eta A}{4l^0} \left(\frac{B_{,i}{}^2 \dot{X}_{i,k}}{B} + \frac{2B_{,i}\, B_{,ik}\, \dot{X}_i}{B} - \frac{B_{,i}{}^2\, B_{,k}\, \dot{X}_i}{B^2} \right) \Bigg] d\xi \ . \end{aligned} \tag{32}$$

Boltzmann model. Using Eqs. (17), (19) and (22), one has

$$\begin{aligned} U = \int_0^1 \Bigg[& \frac{E_1 E_2 A l^0}{2(E_1 + E_2)} \left(\frac{\sqrt{B}}{l^0} - 1 \right)^2 + \int_{X_i} \frac{\eta A E_1}{4l^0 (E_1 + E_2)} \left(\frac{B_{,i}{}^2}{B} \right) \dot{X}_i dX_i + \\ & - \int_{X_i} \frac{\eta A}{2l^0 (E_1 + E_2)} \left(\frac{B_{,i}}{\sqrt{B}} \right) \dot{\sigma} dX_i \Bigg] d\xi \ , \end{aligned} \tag{33}$$

$$\begin{aligned} U_{,i} = \int_0^1 \Bigg[& \frac{E_1 E_2 A}{2(E_1 + E_2)} \left(\frac{B_{,i}}{l^0} - \frac{B_{,i}}{\sqrt{B}} \right) + \frac{\eta A E_1}{4l^0 (E_1 + E_2)} \left(\frac{B_{,i}{}^2}{B} \right) \dot{X}_i + \\ & - \frac{\eta A}{2l^0 (E_1 + E_2)} \left(\frac{B_{,i}}{\sqrt{B}} \right) \dot{\sigma} \Bigg] d\xi \ , \end{aligned} \tag{34}$$

$$\begin{aligned} U_{,ik} = \int_0^1 \Bigg[& \frac{E_1 E_2 A}{2(E_1 + E_2)} \left(\frac{B_{,i}\, B_{,k}}{2B\sqrt{B}} + \frac{B_{,ik}}{l^0} - \frac{B_{,ik}}{\sqrt{B}} \right) + \\ & + \frac{\eta A E_1}{4l^0 (E_1 + E_2)} \left(\frac{B_{,i}{}^2 \dot{X}_{i,k}}{B} + \frac{2B_{,i}\, B_{,ik}\, \dot{X}_i}{B} - \frac{B_{,i}{}^2\, B_{,k}\, \dot{X}_i}{B^2} \right) + \\ & - \frac{\eta A}{2l^0 (E_1 + E_2)} \left(\frac{B_{,ik}}{\sqrt{B}} - \frac{B_{,i}\, B_{,k}}{2B\sqrt{B}} \right) \dot{\sigma} \Bigg] d\xi \ . \end{aligned} \tag{35}$$

Zener model. Using Eqs. (17), (19) and (23), one has

$$U = \int_0^1 \left[\frac{E_1 A l^0}{2} \left(\frac{\sqrt{B}}{l^0} - 1 \right)^2 + \int_{X_i} \frac{\eta A (E_1 + E_2)}{4 l^0 E_2} \left(\frac{B_{,i}{}^2}{B} \right) \dot{X}_i dX_i + \right.$$
$$\left. - \int_{X_i} \frac{\eta A}{2 l^0 E_2} \left(\frac{B_{,i}}{\sqrt{B}} \right) \dot{\sigma} dX_i \right] d\xi \, , \tag{36}$$

$$U_{,i} = \int_0^1 \left[\frac{E_1 A}{2} \left(\frac{B_{,i}}{l^0} - \frac{B_{,i}}{\sqrt{B}} \right) + \frac{\eta A (E_1 + E_2)}{4 l^0 E_2} \left(\frac{B_{,i}{}^2}{B} \right) \dot{X}_i - \frac{\eta A}{2 l^0 E_2} \left(\frac{B_{,i}}{\sqrt{B}} \right) \dot{\sigma} \right] d\xi \, , \tag{37}$$

$$U_{,ik} = \int_0^1 \left[\frac{E_1 A}{2} \left(\frac{B_{,i} B_{,k}}{2B\sqrt{B}} + \frac{B_{,ik}}{l^0} - \frac{B_{,ik}}{\sqrt{B}} \right) + \right.$$
$$+ \frac{\eta A (E_1 + E_2)}{4 l^0 E_2} \left(\frac{B_{,i}{}^2 \dot{X}_{i,k}}{B} + \frac{2 B_{,i} B_{,ik} \dot{X}_i}{B} - \frac{B_{,i}{}^2 B_{,k} \dot{X}_i}{B^2} \right) + \tag{38}$$
$$\left. - \frac{\eta A}{2 l^0 E_2} \left(\frac{B_{,ik}}{\sqrt{B}} - \frac{B_{,i} B_{,k}}{2B\sqrt{B}} \right) \dot{\sigma} \right] d\xi \, .$$

4 NUMERICAL EXAMPLES AND ANALYSIS OF RESULTS

The expressions for the total strain energy and its derivatives stated in item 3.2, for each rheological model, were implemented using the Positional Finite Element Method according to the formulation described in item 2. These formulation and implementation were developed to describe the creep viscoelastic behavior (strain variation over time when exposed to constant stress) due to the application of a static loading (inertial forces are not considered) in space truss finite elements adopting several rheological models.

In item 4.1 a simple example is performed in order to confirm the capacity of the Positional Finite Element Method to describe different creep behaviors through the adoption of appropriate rheological relation. In this example a bar under traction is analyzed using the implementations developed with each model. Furthermore, in item 4.2 a star dome is analyzed to demonstrate the possibility of analysis of more complex space truss structures with the formulations presented.

In the presented analyses below, the terms regarding the rate of stress $\dot{\sigma}$ in Eqs. (27 - 38) are neglected. This approximation is valid for the study of creep behavior, in which the stress is kept constant over time. For relaxation, this approach would not be valid because, in this case, the deformation is taken as constant and the stress is varying in time.

4.1 Bar under traction

In this example a simple structure is analyzed using the implementations developed with each rheological model. This structure is a straight bar with constant cross-section area equal to 1×10^{-4} m^2 and unity length. It is subjected to a static and constant axial tensile stress by means of a static traction load p. This load is applied in one single step and has intensity of 100,000 N. It is applied statically and the creep analysis is considered with this load already applied and stabilized (inertial forces are not considered). This creep analysis is performed considering 150 steps of time of Δt = 100 seconds, coming to a total of 15,000 seconds. The discretization is performed by one truss element with two nodes in which one node is clamped and the other can translate in the x-direction, as shown in Fig. 3.

Figure 3: Bar under traction

The material parameters are chosen so that all models exhibit the same strain at 10,000 seconds, and are presented in Table 1.

Table 1: Material parameters for each rheological model (bar under traction)

Model	η [GPa·s]	E [GPa]	E_1 [GPa]	E_2 [GPa]
Maxwell	3.14×10^5	100.0	–	–
Kelvin-Voigt	1.33×10^5	17.5	–	–
Boltzmann	6.25×10^5	–	25.0	100.0
Zener	1.00×10^5	–	20.0	80.0
Elastic	–	23.9	–	–
Viscous	2.39×10^5	–	–	–

The results of the numerical analyzes are showed in Fig. 4. In which, the evolutions of axial strain over time are presented for each model. In addition, the results for elastic (a single spring) and viscous (a single dashpot) models were included, as showed in Fig. 4.

It is possible to observe from Fig. 4 that the proposed formulations based on Positional Finite Element Method and on rheological models were able to describe different creep viscoelastic behaviors. The evolutions of the axial strain remained as expected by the theory of viscoelasticity presenting intermediate mechanical behavior between purely elastic and purely viscous behavior. Furthermore, Boltzmann, Zener and Maxwell models showed instantaneous elastic strains and appropriate strain profiles over time. On the other hand, Kelvin-Voigt model not showed instantaneous elastic strain, as expected. Moreover, it is important to note that Boltzmann and Zener models can describe the same behavior by means a proper choice of the material parameters.

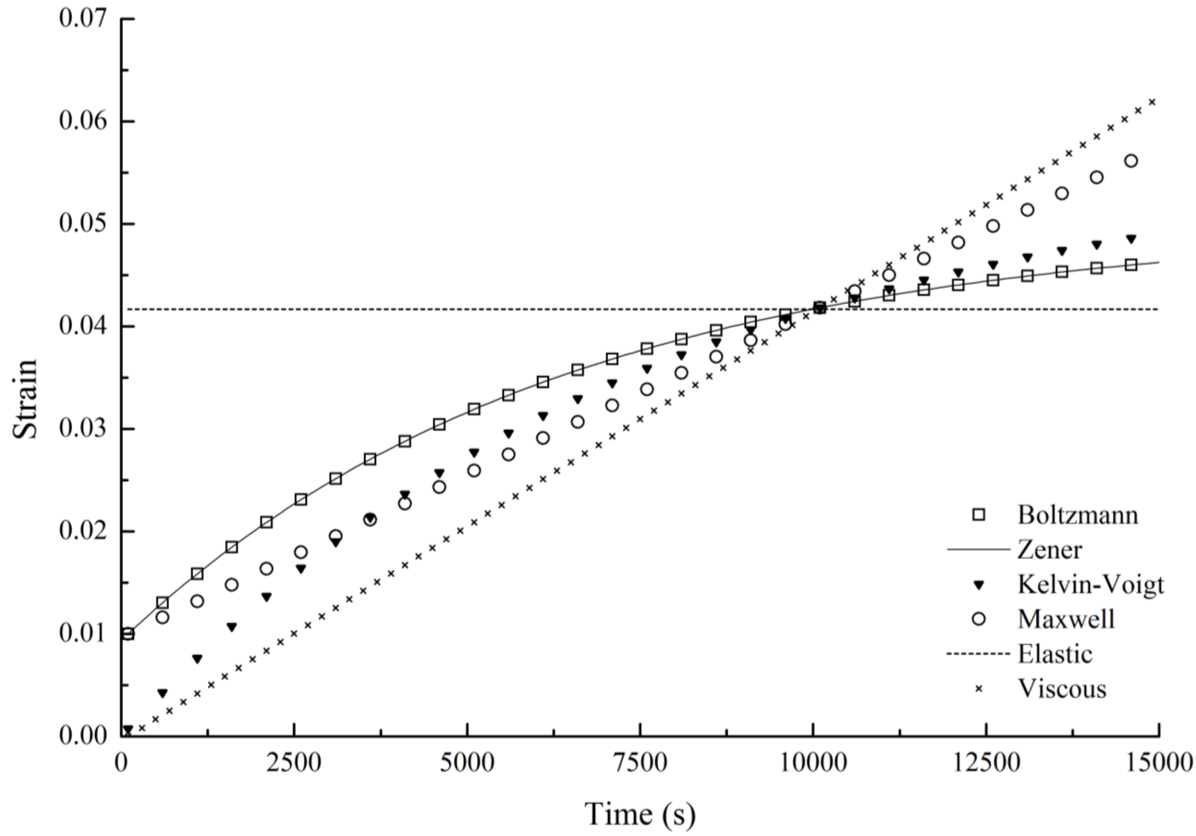

Figure 4: Evolutions of axial strain over time for each model

4.2 Star dome truss

In this example a star dome truss is analyzed to demonstrate the possibility of analysis of more complex space truss structures with the formulations presented for each rheological model. This structure is a typical truss subjected to the instability phenomenon known as snap-through and is very common in the specialized literature about nonlinear analysis, e.g., Greco and Venturini (2006), Krishnamoorthy *et al*. (1996) and Hill *et al*. (1989). The geometry and loading are presented in Fig. 5 with co-ordinates given in cm. To run this example, twenty four elements (13 nodes) are used and 200 steps of 0.1 cm are applied in the central node at the top of the crown. For each member, constant cross-section area equal to 3.17 cm^2 is considered.

The adopted material parameters for each model are presented in Table 2. Boltzmann and Zener parameters are chosen so that the two models exhibit the same equilibrium path. Furthermore, with these parameters the two models show instantaneous elastic behavior like as the elastic model. Kelvin-Voigt parameters are chosen so that, for a sufficiently large period of time, the damped elastic strain tends to the instantaneous elastic strain response expected by a linear elastic model. Finally, the parameters chosen for the Maxwell model are the same as those adopted in the Kelvin-Voigt model.

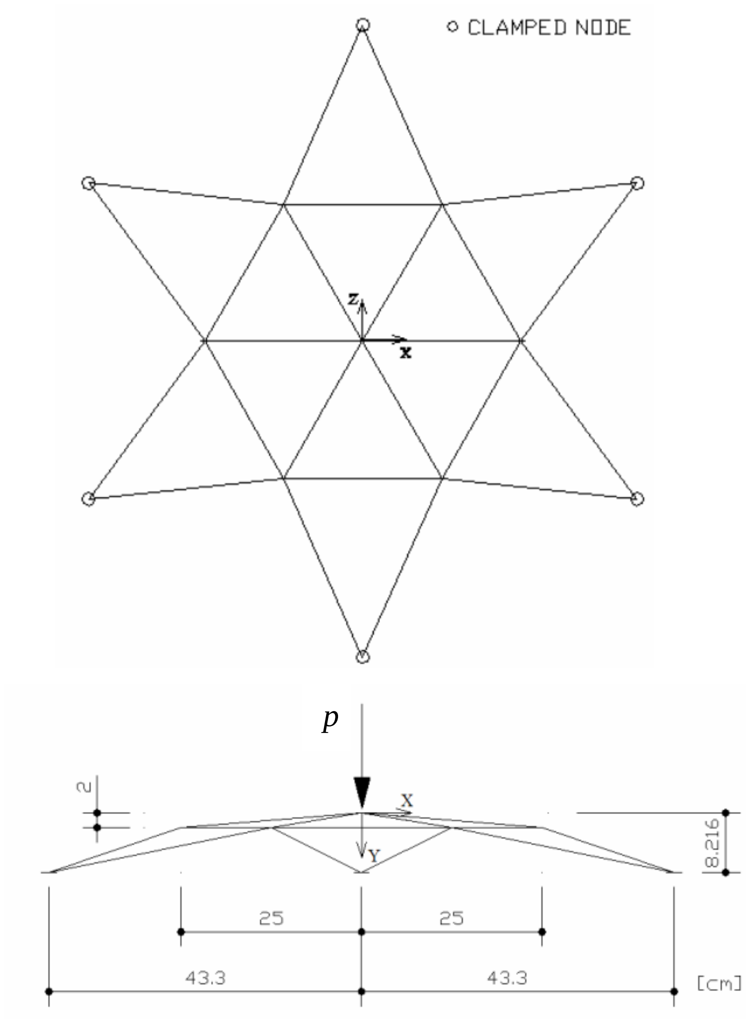

Figure 5: Star dome front and top views (Greco and Venturini, 2006)

Table 2: Material parameters for each rheological model (star dome truss)

Model	η [MPa·s]	E [GPa]	E_1 [GPa]	E_2 [GPa]
Maxwell	10.0	3.0	–	–
Kelvin-Voigt	10.0	3.0	–	–
Boltzmann	62.5	–	4.5	3.0
Zener	10.0	–	1.2	1.8
Elastic	–	3.0	–	–

The results of the numerical analyzes are showed in Fig. 6. In this figure, the central node equilibrium paths are presented for each model. In addition, the results for elastic model (a single spring) obtained from Greco and Venturini (2006) were included, as showed in Fig. 6.

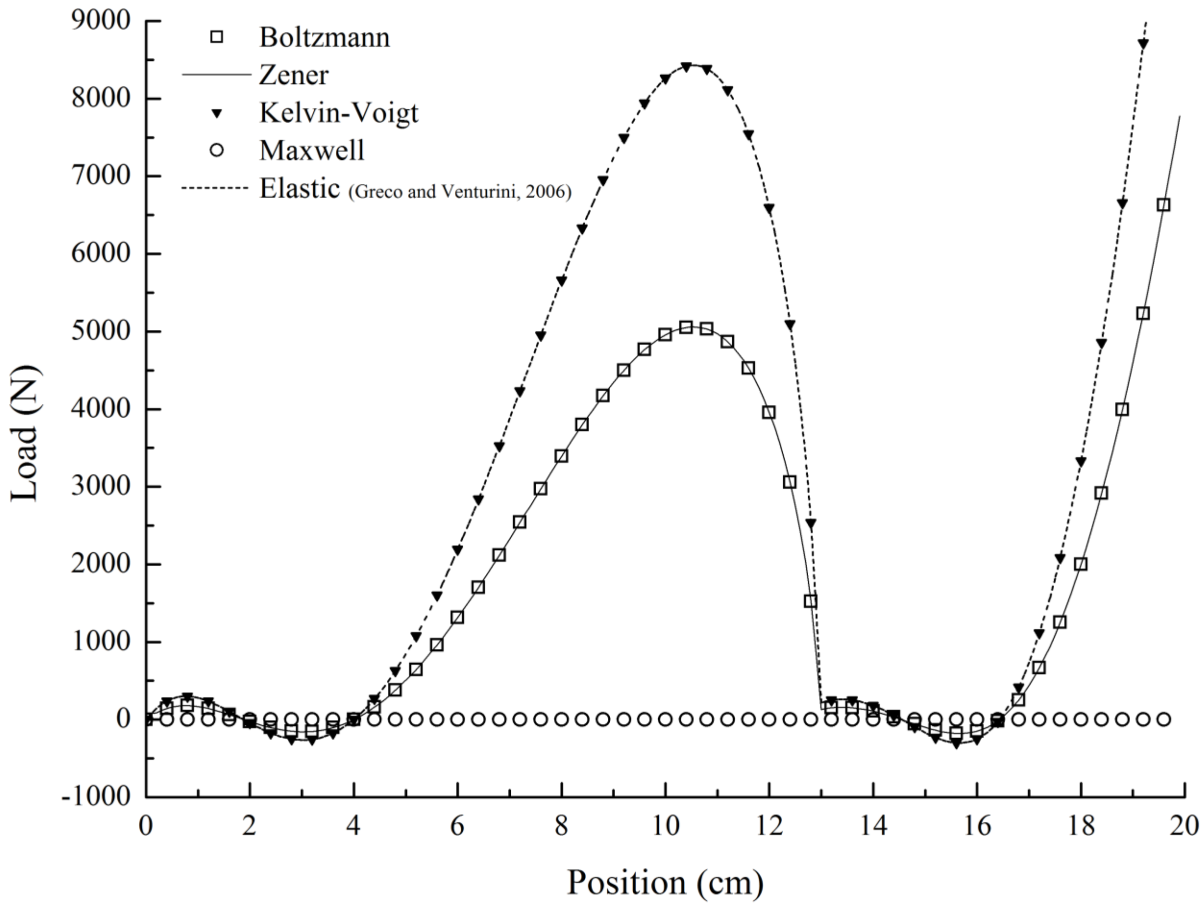

Figure 6: Equilibrium path for central node (prescribed vertical position)

It is possible to observe from Fig. 6 that the proposed formulations based on Positional Finite Element Method and on rheological models were able to describe different viscoelastic behaviors of complex truss structures with accentuated geometric nonlinearity. The central node equilibrium paths remained as expected by the theory of viscoelasticity and in agreement with the strain-time profiles obtained in Fig. 4.

It is important to note from Fig. 6 that Boltzmann and Zener models can describe the same behavior by means a proper choice of the material parameters. Furthermore, these models were able to describe the creep behavior presenting additional viscoelastic strain. Consequently, for these models the equilibrium position was reached with lower loading levels.

As expected, the Kelvin-Voigt model was not able to describe the creep behavior, describing a damped elastic behavior. Thus, in the Fig 6 the damped elastic response obtained is the same of the instantaneous elastic response of the elastic model, since sufficient large period of time has been given to reach the structure equilibrium for each prescribed position.

Finally, for the Maxwell model, the structure equilibrium positions were obtained for loads slightly above zero, as shown in Fig. 6. This result is in agreement with the strain-time profile shown in Fig. 4. This model describes an instantaneous elastic behavior followed by a viscoelastic behavior with constant strain rate, typical of fluid materials. Numerically, the viscoelastic strain increase indefinitely. Thus, low load levels can lead to large displacements of the structure, since sufficient large period of time has been given to reach the structure equilibrium for each prescribed position.

5 CONCLUSIONS AND CLOSING REMARKS

The purpose of this work was to present the formulation and the implementation of different rheological models to describe the creep behavior in space truss elements. This presented formulation was based on the Positional Finite Elements Method. The formulation was applied in a relatively simple way, since it is based on physical concepts of Total Potential Energy balance, which make it easy to understand. The viscoelastic behavior was introduced in a natural way through the implementation of rheological models for obtaining the Total Deformation Energy, since this relation is based on the physical behavior of springs and dashpots associations that provides equations known as phenomenological.

From the results obtained in the presented examples, the formulation was capable to represent the evolution of the strains of the truss elements over time under static load, presenting strain-time profiles for each implemented rheological model as expected from the theory of viscoelasticity. These results confirm the capacity of the Positional Finite Element Method to describe different creep behaviors for different viscoelastic materials, through the adoption of appropriate rheological relation. The analysis of a structure with accentuated geometric nonlinearity demonstrated the viscoelastic model influence and showed that the proposed approach is able to describe different viscoelastic behaviors of complex truss structures. Furthermore, it opens new possibilities to implement more complex models to describe the complex behavior of real materials, such as composite materials, polymeric materials, biological tissues, among others.

ACKNOWLEDGEMENTS

The authors would like to acknowledge CNPq (National Council of Scientific and Technological Development), CAPES (Coordination of Improvement of Higher Education Personnel), FAPEMIG (Minas Gerais State Research Foundation) and PROPEEs/UFMG (Structure Engineering Graduate Program of the Federal University of Minas Gerais) for financial supports.

REFERENCES

Becho, J. S., Barros, F. B., & Greco, M., 2015. Positional formulation for creep mechanical behavior of beams and framed structures. *Science and Engineering Journal*, v. 24, n. 1, p. 31-41. (in Portuguese)

Becho, J. S., Rabelo, J. M. G., Barros, F. B., & Greco, M., 2016. Simulação numérica do comportamento mecânico viscoelástico de fluência em barras de PEAD utilizando a formulação posicional do MEF. In: *XII Simpósio de Mecânica Computacional*. Diamantina, Brazil. (in Portuguese)

Carniel, T. A., Muñoz-Rojas, P. A., & Vaz, M., 2015. A viscoelastic viscoplastic constitutive model including mechanical degradation: Uniaxial transient finite element formulation at finite strains and application to space truss structures. *Applied Mathematical Modelling*, v. 39, n. 5, p. 1725-1739.

Crisfield, M. A., 2003. *Non-linear finite element analysis of solids and structures*. v.1. John Wiley & Sons, West Sussex.

Dym, C. L., & Shames, I. H., 2013. *Solid mechanics: a variational approach*. Springer, New York.

Findley, W. N., Lai, J. S., & Onaran, K., 1989. *Creep and relaxation of nonlinear viscoelastic materials*. Dover Publications, New York.

Godat, A., Légeron, F., Gagné, V., & Marmion, B., 2013. Use of FRP pultruded members for electricity transmission towers. *Composite Structures*, v. 105, p. 408-421.

Greco, M., Gesualdo, F. A. R., Venturini, W. S., & Coda, H. B., 2006. Nonlinear positional formulation for space truss analysis. *Finite Element in Analysis and Design*, v.42, n. 12, p.1079-1086.

Greco, M., & Venturini, W. S., 2006. Stability analysis of three-dimensional trusses. *Latin American Journal of Solids and Structures*, v. 3, n. 3, p. 325-344.

Hill, C. D., Blandford, G. E., & Wang, S. T., 1989. Post-buckling analysis of steel space trusses. *Journal of Structural Engineering*, v. 115, n. 4, p. 900-919.

Kaliske, M., & Rothert, H., 1997. Formulation and implementation of three-dimensional viscoelasticity at small and finite strains. *Computational Mechanics*, v. 19, n. 3, p. 228-239.

Kästner, M., Obst, M., Brummund, J., Thielsch, K., & Ulbricht, V., 2012. Inelastic material behavior of polymers–experimental characterization, formulation and implementation of a material model. *Mechanics of Materials*, v. 52, p. 40-57.

Krishnamoorthy, C. S., Ramesh, G., & Dinesh, K. U., 1996. Post-buckling analysis of structures by three-parameter constrained solution techniques. *Finite elements in analysis and design*, v. 22, n. 2, p. 109-142.

Kühl, A., Muñoz-Rojas, P. A., Barbieri, R., & Benvenutti, I. J., 2016. A procedure for modeling the nonlinear viscoelastoplastic creep of HDPE at small strains. *Polymer Engineering and Science*, v. 57, n. 2, p. 144-152.

Liu, H., Polak, M., & Penlidis, A., 2008. A practical approach to modeling time-dependent nonlinear creep behavior of polyethylene for Structural applications. *Polymer Engineering and Science*, v. 48, n. 1, p. 159-167.

Marques, S. P. C., & Creus, G. J., 2012. *Computational viscoelasticity*. Springer, Heidelberg.

Mesquita, A. D., & Coda, H. B., 2003. A simple Kelvin and Boltzmann viscoelastic analysis of three-dimensional solids by the boundary element method. *Engineering Analysis with Boundary Elements*, v. 27, n. 9, p. 885-895.

Muñoz-Rojas, P. A., Mendonça, P. T. R., Benvenutti, I. J., & Creus, G. J., 2011. Modeling nonlinear viscoelastic behavior of High Density Polyethylene (HDPE): application of stress-time equivalence versus interpolation of rheological properties. In: *III International Symposium on Solid Mechanics*. Florianópolis, Brazil.

Ogden, R. W., 1997. *Non-linear elastic deformation*. Chichester, Ellis Horwood.

Panagiotopoulos, C. G., Mantič, V., & Roubíček, T., 2014. A simple and efficient BEM implementation of quasistatic linear visco-elasticity. *International Journal of Solids and Structures*, v. 51, n. 13, p. 2261-2271.

Sá, M. F., Gomes, A. M.,Correia, J. R., & Silvestre, N., 2011. Creep behavior of pultruded GFRP elements–Part 1: Literature review and experimental study. *Composite Structures*, v. 93, n. 10, p. 2450-2459.

Semptikovski, S. C., & Muñoz-Rojas, P. A., 2013. A Geometrically Nonlinear Simplified Beam Element with Linear Viscoelastic Behaviour. In: *IV International Symposium on Solid Mechanics*, Porto Alegre, Brazil.